# Closed-Form Direction-Finding with Arbitrarily Spaced Electromagnetic Vector-Sensors at Unknown Locations †

*Paper Category: 5.3 Array Signal Processing*

Kainam Thomas Wong
*Nanyang Technological University,*
*School of Electrical & Electronic Engineering,*
*Nanyang Avenue, Singapore 639798*
*ktwong@mailexcite.com*

Michael D. Zoltowski
*Purdue University,*
*School of Electrical & Computer Engineering,*
*West Lafayette, IN 47907-1285 U.S.A.*
*mikedz@ecn.purdue.edu*

## ABSTRACT

This paper introduces a novel closed-form ESPRIT-based algorithm for multi-source direction finding using arbitrarily spaced electromagnetic vector-sensors whose locations need *not* be known. The electromagnetic vector-sensor, already commercially available, consists of six co-located but diversely polarized antennas separately measuring all six electromagnetic-field components of an incident wavefield. In this novel algorithm, ESPRIT exploits the non-spatial inter-relations among the six unknown electromagnetic-field components of each source and produces from the measured data a set of eigenvalues, from which the source's electromagnetic-field vector may be estimated to within a complex scalar. Application of a vector cross-product operation to this ambiguous electromagnetic-field vector estimate produces an unambiguous estimate of that source's normalized Poynting-vector, which contains as its components the source's Cartesian direction-cosines. Monte Carlo simulation results verify the efficacy and versatility of this innovative scheme.

## 1. INTRODUCTION

ESPRIT (Estimation of Signal Parameters via Rotational Invariance Techniques [2]) represents a highly popular eigenstructure (subspace) parameter estimation method. ESPRIT requires a certain invariance structure in the sampled data set; and this invariance structure has generally been realized in most ESPRIT-based direction-finding (DF) algorithms as a *spatial* invariance dependent on some known translational displacement ($\Delta$) between two identical subarrays of sensors. This spatial-invariance relates the two subarrays' responses to the $k$th impinging source through an invariant phase-factor $e^{j2\pi\frac{\Delta}{\lambda}u(\theta_k,\phi_k)}$, where $\lambda$ denotes the signal wavelength and $u(\theta_k,\phi_k)$ represents the $k$th source's direction-cosine parameterized by the elevation angle $\theta_k$ and the azimuth angle $\phi_k$. Thus, estimation of this invariant phase-factor would yield an estimate of the $k$th source's direction-cosine (and hence its direction-of-arrival).

In contrast, this proposed algorithm advances a *non-spatial* realization of ESPRIT's invariance structure, such that the invariance factors would depend only on the impinging signals' direction-cosines and not on array geometry. This proposed algorithm also offers closed-form solutions for any irregular and even possibly *un*known array geometry, whereas most other algorithms would require iterative searches (such as the MUSIC algorithm [1]) to handle arbitrary and a priori *known* array geometry. As a consequence, this proposed algorithm (1) is computationally less intensive than many open-form search methods, (2) requires no a priori coarse estimates of the arrival angle to start off any iterative search, (3) requires no a priori detailed calibrated knowledge and computer storage of the array manifold, (4) makes possible sparse array aperture extension while producing closed-form unambiguous arrival angle estimation with no extra computation needed for disambiguation. Because this novel algorithm is also highly parallel in its computational structure, concurrent computer processing facilitates real-time implementations.

This novel scheme employs electromagnetic vector-sensors, each of which consists of six spatially co-located but diversely polarized antennas, separately measuring all three electrical-field components and all three magnetic-field components of the incident wave-field. Electromagnetic vector-sensors can exploit any polarization diversity among the impinging radar sources. Sources impinging upon the array from the same angular directions can thus be resolved on account of their distinct polarization states, thereby enhancing performance. Electromagnetic vector-sensors are already commercially available, for example from Flam and Russell Inc. in Horsham, Pennsylvania, U.S.A. [3] and from EMC Baden Inc. in Baden, Switzerland.

The first direction-finding algorithms explicitly exploiting all six electromagnetic components appear to have been developed separately by Nehorai & Paldi [4] and Jian Li [5]. Nehorai & Paldi [4], who coined the term "vector-sensor", pioneered the simple but novel idea of using the vector cross-product of the electric-field vector estimate and the magnetic-field vector estimate (provided the vector-sensor outputs) to estimate directly the two-dimensional radial direction of a source. This vector cross-product angle estimator has been applied to eigenstructure-based direction finding by Wong & Zoltowski in [7-11]. Whereas the multiple vector-sensor direction finding algorithms of [7,9-11] require a priori knowledge of array geometry, this proposed algorithm does not.

This present paper may be considered as an elegant and simplified improvement of Jian Li's ESPRIT-based algorithm [5] for magnetic loops and electric dipoles. Like [5] but unlike [7-11], the present algorithm considers the $L$ vector-sensors (with their $6L$ components) as six co-located subarrays, each of which comprises identically polarized antennas but among which the polarization is diverse. Like [5], the present algorithm applies ESPRIT multiple times to distinct pairs of these six subarrays to extract the invariant factors characterizing the six electromagnetic-field components of the impinging sources. The pivotal insight of this paper is that five invariant factors relating the six electromagnetic-field components suffice for unique determination of the source's normalized Poynting vector and thus the source's arrival angles. That is, these five invariant factors would produce an ambiguous estimate of each

†This research work was supported by the U.S. National Science Foundation under grant no. MIPS-9320890, the U.S. AFOSR under contract no. F49620-95-1-0367, and the U.S. Army Research Office Focused Research Initiative under grant no. DAAH04-95-1-0246.

impinging source's electromagnetic-field vector, correct to within a complex scalar. This electromagnetic-field vector estimate, though ambiguous, can produce an unambiguous estimate of the source's normalized Poynting vector via a vector cross-product. This algorithm thus substitutes the elegant and simple operation of a vector cross product for the complex manipulation in [5] involving a set of highly non-linear equations. That both the present algorithm and [5] do not require any a priori knowledge of the location of any of the vector-sensors is because the aforementioned invariant factors depend only on the source parameters but not on the vector-sensors' spatial locations.

## 2. MATHEMATICAL DATA MODEL

Uncorrelated transverse electromagnetic plane-waves, having traveled through a homogeneous isotropic medium, impinge upon a three-dimensional array of arbitrarily spaced but identically oriented electromagnetic vector-sensors at possibly unknown spatial locations. This identical orientation assumption will be relaxed in the journal version of this work. The $k$th such unit-power incident source has the array manifold [4,5]: $\mathbf{a}(\theta_k, \phi_k, \gamma_k, \eta_k)$

$$\stackrel{\text{def}}{=} \begin{bmatrix} \mathbf{e}_k \\ \mathbf{h}_k \end{bmatrix} \stackrel{\text{def}}{=} \begin{bmatrix} e_{x_k} \\ e_{y_k} \\ e_{z_k} \\ h_{x_k} \\ h_{y_k} \\ h_{z_k} \end{bmatrix} \stackrel{\text{def}}{=} \begin{bmatrix} a_1(\theta_k, \phi_k, \gamma_k, \eta_k) \\ a_2(\theta_k, \phi_k, \gamma_k, \eta_k) \\ a_3(\theta_k, \phi_k, \gamma_k, \eta_k) \\ a_4(\theta_k, \phi_k, \gamma_k, \eta_k) \\ a_5(\theta_k, \phi_k, \gamma_k, \eta_k) \\ a_6(\theta_k, \phi_k, \gamma_k, \eta_k) \end{bmatrix} \quad (1)$$

$$= \underbrace{\begin{bmatrix} \cos\phi_k \cos\theta_k & -\sin\phi_k \\ \sin\phi_k \cos\theta_k & \cos\phi_k \\ -\sin\theta_k & 0 \\ -\sin\phi_k & -\cos\phi_k\cos\theta_k \\ \cos\phi_k & -\sin\phi_k \cos\theta_k \\ 0 & \sin\theta_k \end{bmatrix}}_{\stackrel{\text{def}}{=}\boldsymbol{\Theta}_k} \underbrace{\begin{bmatrix} \sin\gamma_k \, e^{j\eta_k} \\ \cos\gamma_k \end{bmatrix}}_{\stackrel{\text{def}}{=}\mathbf{g}_k} \quad (2)$$

where $0 \leq \theta_k < \pi$ denotes the signal's elevation angle measured from the vertical z-axis, $0 \leq \phi_k < 2\pi$ signifies the azimuth angle, $0 \leq \gamma_k < \pi/2$ represents the auxiliary polarization angle and $-\pi \leq \eta_k < \pi$ symbolizes the polarization phase difference, The electric-field vector $\mathbf{e}_k$ and the magnetic-field vector $\mathbf{h}_k$ are orthogonal to each other and to the $k$th source's direction of propagation; i.e., the normalized Poynting-Vector $\mathbf{p}_k$:

$$\begin{aligned} \mathbf{p}_k &\stackrel{\text{def}}{=} \begin{bmatrix} p_{x_k}(\theta_k,\phi_k) \\ p_{y_k}(\theta_k,\phi_k) \\ p_{z_k}(\theta_k,\phi_k) \end{bmatrix} \stackrel{\text{def}}{=} \begin{bmatrix} u_k \\ v_k \\ w_k \end{bmatrix} = \begin{bmatrix} \sin\theta_k \, \cos\phi_k \\ \sin\theta_k \, \sin\phi_k \\ \cos\theta_k \end{bmatrix} \\ &= \mathbf{e}_k(\theta_k, \phi_k, \gamma_k, \eta_k) \times \mathbf{h}_k^*(\theta_k, \phi_k, \gamma_k, \eta_k) \quad (3) \end{aligned}$$

where $^*$ denotes complex conjugation, $u_k, v_k$ and $w_k$ denote respectively the direction-cosine along the x-, y- and z-axes. Whilst the above electromagnetic vector-sensor model has not accounted for mutual coupling among the electromagnetic vector-sensor's six component-antennas, this model has been reported by Flam & Russell Inc. to be a very good approximation of their CART array implementation of the electromagnetic vector-sensor concept.[1]

The inter-vector-sensor spatial phase-factor relating the $k$th source to the $l$th electromagnetic vector-sensor at the (possibly unknown) location $(x_l, y_l, z_l)$ is:

$$q_l(\theta_k, \phi_k) \stackrel{\text{def}}{=} e^{j2\pi\frac{x_l u_k}{\lambda}} e^{j2\pi\frac{y_l v_k}{\lambda}} e^{j2\pi\frac{z_l w_k}{\lambda}} \quad (4)$$

[1] "...the patterns of the loops and dipoles [of the CART array] are EXTREMELY close to the theoretical patterns, indicating very good isolation and balance among the elements."—private correspondence from Mr. Richard Flam of Flam & Russell to the first author on January 15, 1997.

The $6L \times 1$ array manifold for the entire $L$-element vector-sensor array is:

$$\begin{aligned} \mathbf{a}^{(L)}(\theta_k, \phi_k, \gamma_k, \eta_k) &\stackrel{\text{def}}{=} \mathbf{a}(\theta_k, \phi_k, \gamma_k, \eta_k) \otimes \mathbf{q}(\theta_k, \phi_k) \\ \mathbf{q}(\theta_k, \phi_k) &\stackrel{\text{def}}{=} \mathbf{q}(u(\theta_k,\phi_k), v(\theta_k,\phi_k)) \\ &= \begin{bmatrix} q_1(\theta_k,\phi_k) \\ \vdots \\ q_L(\theta_k,\phi_k) \end{bmatrix} \end{aligned}$$

where $\otimes$ symbolizes the Kronecker-product operator.

With a total of $K \leq L$ co-channel signals, the entire array would yield a $6L \times 1$ vector measurement $\mathbf{z}(t)$ at times $t$:

$$\mathbf{z}(t) = \sum_{k=1}^{K} \mathbf{a}^{(L)}(\theta_k, \phi_k, \gamma_l, \eta_l) s_k(t) + \mathbf{n}(t) = \mathbf{A}\mathbf{s}(t) + \mathbf{n}(t)$$

with

$$\begin{aligned} s_k(t) &\stackrel{\text{def}}{=} \sqrt{\mathcal{P}_k}\sigma_k(t) e^{j(2\pi\frac{c}{\lambda}t + \varphi_k)} \\ \mathbf{A} &\stackrel{\text{def}}{=} [\mathbf{a}^{(L)}(\theta_1,\phi_1,\gamma_1,\eta_1), \cdots, \mathbf{a}^{(L)}(\theta_K,\phi_K,\gamma_K,\eta_K)] \\ \mathbf{s}(t) &\stackrel{\text{def}}{=} \begin{bmatrix} s_1(t) \\ \vdots \\ s_K(t) \end{bmatrix}; \qquad \mathbf{n}(t) \stackrel{\text{def}}{=} \begin{bmatrix} n_1(t) \\ \vdots \\ n_{6L}(t) \end{bmatrix} \end{aligned}$$

and $\mathbf{n}(t)$ symbolizes the $6L \times 1$ additive zero-mean white noise vector, $\mathcal{P}_k$ denotes the $k$th signal's power, $\sigma_k(t)$ represents a zero-mean unit-variance complex random process, $\lambda$ refers to the signals' wavelength, $c$ signifies the propagation speed, and $\varphi_k$ denotes the $k$th signal's uniformly-distributed random carrier phase.

With a total of $N$ (with $N > K$) snapshots taken at the distinct instances $\{t_n, \ n = 1, \ldots, N\}$, the present direction-finding problem is to determine $\{\theta_k, \phi_k, \ k = 1, \ldots, K\}$ from the $6L \times N$ data set: $\mathbf{Z} \stackrel{\text{def}}{=} [\ \mathbf{z}(t_1) \ \ \ldots \ \ \mathbf{z}(t_N)\ ]$ without knowledge of $\mathbf{q}(\theta_k, \phi_k)$. [2]

## 3. DF WITH ARBITRARILY SPACED VECTOR-SENSORS AT UNKNOWN LOCATIONS

### 3.1. Overview of Algorithm

The pivotal insight underlying the present algorithm is that the $6L \times 1$ array manifold may be divided into six $(L \times 1)$ subarray manifolds, which are related by invariant factors dependent only on the inter-relation among the six electromagnetic-field components of each source's direction-cosines but not on the vector-sensor's spatial locations. To be precise, the $6L \times 1$ array manifold $\mathbf{a}^{(L)}(\theta_k, \phi_k, \gamma_k, \eta_k) = \mathbf{a}(\theta_k, \phi_k, \gamma_k, \eta_k) \otimes \mathbf{q}(\theta_k, \phi_k)$ may be alternately expressed as:

$$\mathbf{a}^{(L)}(\theta_k, \phi_k, \gamma_k, \eta_k) = \begin{bmatrix} a_1(\theta_k, \phi_k, \gamma_k, \eta_k)\mathbf{q}(\theta_k, \phi_k) \\ a_2(\theta_k, \phi_k, \gamma_k, \eta_k)\mathbf{q}(\theta_k, \phi_k) \\ a_3(\theta_k, \phi_k, \gamma_k, \eta_k)\mathbf{q}(\theta_k, \phi_k) \\ a_4(\theta_k, \phi_k, \gamma_k, \eta_k)\mathbf{q}(\theta_k, \phi_k) \\ a_5(\theta_k, \phi_k, \gamma_k, \eta_k)\mathbf{q}(\theta_k, \phi_k) \\ a_6(\theta_k, \phi_k, \gamma_k, \eta_k)\mathbf{q}(\theta_k, \phi_k) \end{bmatrix}$$

$$\text{with} \quad \mathbf{J}_j \mathbf{a}^{(L)}(\theta_k, \phi_k) \stackrel{\text{def}}{=} a_j(\theta_k, \phi_k, \gamma_k, \eta_k)\mathbf{q}(\theta_k, \phi_k) \quad (5)$$

where $\mathbf{J}_j$ is an $L \times 6L$ subarray selection matrix:

[2] Although the proposed algorithm is herein presented in the batch processing mode, real-time adaptive implementations of this present algorithm may be readily realized for non-stationary environments using the fast recursive eigen-decomposition updating methods such as that in [6].

$$\mathbf{J}_j \stackrel{\text{def}}{=} \left[\mathbf{O}_{L,L\times(j-1)} \vdots \mathbf{I}_L \vdots \mathbf{O}_{L,L\times(6-j)}\right], \qquad j=1,\ldots,6 \quad (6)$$

and $\mathbf{O}_{m,n}$ denotes an $m \times n$ zero matrix and $\mathbf{I}_m$ denotes an $m \times m$ identity matrix. Six $L \times K$ subarray manifolds $\{\mathbf{A}_j,\, j=1,\ldots,6\}$ may thus be formed out of the $6L \times K$ array manifold $\mathbf{A}$:

$$\mathbf{A}_j \stackrel{\text{def}}{=} \mathbf{J}_j\mathbf{A}, \qquad j=1,\ldots,J \quad (7)$$

These $\{\mathbf{A}_1,\ldots,\mathbf{A}_6\}$ subarray manifolds are inter-related as follows:

$$\mathbf{A}_{j+1} = \mathbf{A}_j \underbrace{\begin{bmatrix} \chi_1^{(j,j+1)} & & \\ & \ddots & \\ & & \chi_K^{(j,j+1)} \end{bmatrix}}_{\stackrel{\text{def}}{=}\mathbf{X}^{(j,j+1)}} \quad (8)$$

where $\chi_k^{(j,j+1)} \stackrel{\text{def}}{=} \frac{a_{j+1}(\theta_k,\phi_k,\gamma_k,\eta_k)}{a_j(\theta_k,\phi_k,\gamma_k,\eta_k)}$. In other words, the matrix-pencil $\{\mathbf{A}_j,\mathbf{A}_{j+1}\}$ has generalized eigenvalues equal to $\{\chi_k^{(j,j+1)},\, k=1,\ldots,K\}$. Note that none of $\{\chi^{(j,j+1)},\, k=1,\ldots,K,\, j=1,\ldots,5\}$ depends on the vector-sensors' locations $\{(x_l,y_l,z_l),\, l=1,\ldots,L\}$. The foregoing analysis thus suggests that without any constraint on nor any knowledge of the location of any of the electromagnetic vector-sensors, application of ESPRIT to the matrix-pencil in (8) would estimate the invariant factors $\{\chi_k^{(j,j+1)},\, j=1,\ldots,5\}$ among $k$th source's six electromagnetic-field components, $\{\mathbf{a}_j(\theta_k,\phi_k,\gamma_k,\eta_k),\, j=1,\ldots,6\}$. Note that ESPRIT may be applied to the five matrix-pencils $\{\mathbf{A}_j,\mathbf{A}_{j+1},\quad j=1,\ldots,5\}$ in parallel to facilitate real-time implementation.

### 3.2. Subspace Decomposition

In eigenstructure (subspace) direction-finding methods such as ESPRIT, the overall data correlation matrix $\mathbf{ZZ}^H$ is decomposed into a $K$-dimensional signal subspace and a $(6L-K)$-dimensional noise subspace. Therefore, the first step in the proposed algorithm is to compute the $K$ $(6L\times 1)$ signal-subspace eigenvectors by eigen-decomposing the $6L\times 6L$ data correlation matrix $\mathbf{R}_{zz}=\mathbf{ZZ}^H$. Let $\mathbf{E}_s$ be the $6L\times K$ matrix composed of the $K$ eigenvectors corresponding to the $K$ largest eigenvalues of $\mathbf{R}_{zz}$:

$$\begin{aligned}\mathbf{E}_s \approx \mathbf{AT} = [&\mathbf{a}(\theta_1,\phi_1,\gamma_1,\eta_1)\otimes\mathbf{q}(\theta_1,\phi_1),\cdots,\\ &\mathbf{a}(\theta_K,\phi_K,\gamma_K,\eta_K)\otimes\mathbf{q}(\theta_K,\phi_K)]\,\mathbf{T}\end{aligned} \quad (9)$$

where $\mathbf{T}$ symbolizes an unknown but non-singular $K\times K$ coupling matrix. $\mathbf{T}$ is non-singular because both $\mathbf{E}_s$ and $\mathbf{A}$ are full rank. If there were no noise or if an infinite number of snapshots were available; the approximation would become exact.

### 3.3. Estimation of $\{\chi_k^{(j,j+1)},\, k=1,\ldots,K\}$

Analogous to (8), $\mathbf{J}_j$ and $\mathbf{J}_{j+1}$ are next used to construct the signal-subspace matrix-pencil $\{\mathbf{E}_{s,j},\mathbf{E}_{s,j+1}\}$,

$$\mathbf{E}_{s,j} = \mathbf{J}_j\mathbf{E}_s \approx \mathbf{A}_j\mathbf{T} \quad (10)$$

$$\mathbf{E}_{s,j+1} = \mathbf{J}_{j+1}\mathbf{E}_s \approx \mathbf{A}_{j+1}\mathbf{T} \quad (11)$$

There exists a $K\times K$ non-singular matrix $\mathbf{\Psi}^{(j,J+1)}$ relating the two $L\times K$ full-ranked matrices $\mathbf{E}_{s,j}$ and $\mathbf{E}_{s,j+1}$ [1]:

$$\begin{aligned}\mathbf{E}_{s,j}\mathbf{\Psi}^{(j,j+1)} &= \mathbf{E}_{s,j+1}\\ \Rightarrow\ \mathbf{A}_j\mathbf{T}^{(j,j+1)}\mathbf{\Psi}^{(j,j+1)} &\approx \mathbf{A}_{j+1}\mathbf{T}^{(j,j+1)}\\ \Rightarrow\ \mathbf{\Psi}^{(j,j+1)} &= \left((\mathbf{E}_{s,j})^H\mathbf{E}_{s,j}\right)^{-1}\left((\mathbf{E}_{s,j})^H\mathbf{E}_{s,j+1}\right)\\ \Rightarrow\ \mathbf{\Psi}^{(j,j+1)} &\approx (\mathbf{T}^{(j,j+1)})^{-1}\mathbf{X}^{(j,j+1)}\mathbf{T}^{(j,j+1)}\end{aligned} \quad (12)$$

where $\mathbf{T}^{(j,j+1)}=\mathbf{P}^{(j,j+1)}\mathbf{T}$, and $\mathbf{P}^{(j,j+1)}$ is some unknown permutation matrix whose $k$th column is a $K\times 1$ vector with all zeroes except a one at the $i_k$th position and $\{i_1,\ldots,i_K\}$ is some permutation of $\{1,\ldots,K\}$. This unknown permutation of the rows of $\mathbf{T}$ (i.e. the permutation of the eigenvectors of $\mathbf{\Psi}^{(j,j+1)}$) as columns of $(\mathbf{T}^{(j,j+1)})^{-1}$ arises in the eigen-decomposition of $\mathbf{\Psi}^{(j,j+1)}$—for any $\mathbf{T}$ satisfying (12), $\mathbf{P}^{(j,j+1)}\mathbf{T}$ would likewise satisfy (12). From these, the invariant factor $\chi_k^{(j,j+1)}$ between the $a_{j+1}(\theta_k,\phi_k,\gamma_k,\eta_k)$ and $a_j(\theta_k,\phi_k,\gamma_k,\eta_k)$ may be estimated for each of the $K$ sources:

$$\hat{\chi}_{k(j)}^{(j,j+1)} \approx [\mathbf{X}^{(j,j+1)}]_{kk}, \qquad k=1,\ldots,K \quad (13)$$

where $\{[\mathbf{X}^{(j,j+1)}]_{kk},\quad k=1,\ldots,K\}$ constitute the diagonal elements of the diagonal matrix $\mathbf{X}^{(j,j+1)}$ and are approximated by the eigenvalues of $\mathbf{\Psi}^{(j,j+1)}$. (The reason for the superscript $(j)$ in $k$ will become clear shortly.) Furthermore, the eigenvector corresponding to the eigenvalue $[\mathbf{X}^{(j,j+1)}]_{kk}$ constitutes the $k$th column of $(\mathbf{T}^{(j,j+1)})^{-1}$.

Note that different indices are used to enumerate $\hat{\chi}_k^{(j,j+1)}$ for different values of $j$ and that in general $\mathbf{T}^{(j,j+1)}\neq\mathbf{T}^{(i,i+1)}$ for $j\neq i$, even though $\mathbf{\Psi}^{(j,j+1)}$ and $\mathbf{\Psi}^{(i,i+1)}$ share the same set of eigenvectors. That is, the eigenvectors are ordered differently in $(\mathbf{T}^{(j,j+1)})^{-1}$ as in $(\mathbf{T}^{(i,i+1)})^{-1}$. No mismatch, however, exists between $\hat{\chi}_k^{(j,j+1)}$ and its corresponding eigenvector, namely the $k$th column of $(\mathbf{T}^{(j,j+1)})^{-1}$. This is true for all $j\in\{1,\ldots,5\}$. Thus, $\hat{\chi}_{k(j)}^{(j,j+1)}$ may be paired with $\hat{\chi}_{k(i)}^{(i,i+1)}$ from the same source by matching the orthogonal rows of $\mathbf{T}^{(j,j+1)}$ with those of $\mathbf{T}^{(i,i+1)}$ as follows. Let $(k^{(j)},k^{(i)})$ denote the row-index of the matrix element with the largest absolute value in the $k^{(i)}$-th column of the $K\times K$ matrix $\mathbf{T}^{(i,i+1)}(\mathbf{T}^{(j,j+1)})^{-1}$. Then $\hat{\chi}_{k(j)}$ and $\hat{\chi}_{k(i)}$ belong to the same source. Note that this pairing procedure involves minimum computation and requires *no* exhaustive searches. An alternate pairing method, requiring more computation but offering possibly more robust pairing, is available in [6].

### 3.4. DOA Estimation via Vector-Sensor Product

The algorithm thus far is entirely parallel to that in [5] by Jian Li. With up to $\begin{pmatrix} & 6 & \\ 2 & 2 & 2\end{pmatrix}/3! = 15$ distinct pairings among the six electromagnetic-field components, there are available up to 15 non-linear equations relating the four unknown signal parameters $\{\theta_k,\phi_k,\gamma_k,\eta_k\}$. Li [5] then derived closed-form expressions for these four parameters based on clever but complicated manipulation of these 15 non-linear equations. Instead, the present algorithm will suggest a simpler and more elegant approach based on the recognition that (1) preceding algorithmic steps have already estimated the six-component electromagnetic-field vector to within a complex constant, (2) this result will be sufficient to determine uniquely the corresponding normalized Poynting vector.

Because $\chi_k^{(j,j+1)}$ embodies the ratio between $a_{j+1}(\theta_k,\phi_k,\gamma_k,\eta_k)$ and $a_j(\theta_k,\phi_k,\gamma_k,\eta_k)$, under noiseless conditions:

$$\hat{\mathbf{a}}(\theta_k,\phi_k,\gamma_k,\eta_k) = r_k e^{j\alpha_k}\begin{bmatrix} 1 \\ \chi_k^{(1,2)} \\ \chi_k^{(1,2)}\chi_k^{(2,3)} \\ \chi_k^{(1,2)}\chi_k^{(2,3)}\chi_k^{(3,4)} \\ \chi_k^{(1,2)}\chi_k^{(2,3)}\chi_k^{(3,4)}\chi_k^{(4,5)} \\ \chi_k^{(1,2)}\chi_k^{(2,3)}\chi_k^{(3,4)}\chi_k^{(4,5)}\chi_k^{(5,6)}\end{bmatrix} \quad (14)$$

where $r_k$ represents a real scalar, $0 \leq \alpha_k < 2\pi$, and $r_k e^{j\alpha_k} = e_{x_k}$. Thus, under noisy conditions $\hat{\mathbf{p}}_k$ equals

$$\|r_k\|^2 \begin{bmatrix} 1 \\ \chi_k^{(1,2)} \\ \chi_k^{(1,2)}\chi_k^{(2,3)} \end{bmatrix} \times \begin{bmatrix} \chi_k^{(1,2)}\chi_k^{(2,3)}\chi_k^{(3,4)} \\ \chi_k^{(1,2)}\chi_k^{(2,3)}\chi_k^{(3,4)}\chi_k^{(4,5)} \\ \chi_k^{(1,2)}\chi_k^{(2,3)}\chi_k^{(3,4)}\chi_k^{(4,5)}\chi_k^{(5,6)} \end{bmatrix}^*$$

However because $\mathcal{P}_k = 1$, the $k$th impinging source's Cartesian direction-cosine estimates, $[\hat{u}_k, \hat{v}_k, \hat{w}_k]^T$, equal:

$$\frac{\begin{bmatrix} 1 \\ \chi_k^{(1,2)} \\ \chi_k^{(1,2)}\chi_k^{(2,3)} \end{bmatrix} \times \begin{bmatrix} \chi_k^{(1,2)}\chi_k^{(2,3)}\chi_k^{(3,4)} \\ \chi_k^{(1,2)}\chi_k^{(2,3)}\chi_k^{(3,4)}\chi_k^{(4,5)} \\ \chi_k^{(1,2)}\chi_k^{(2,3)}\chi_k^{(3,4)}\chi_k^{(4,5)}\chi_k^{(5,6)} \end{bmatrix}^*}{\left\| \begin{bmatrix} 1 \\ \chi_k^{(1,2)} \\ \chi_k^{(1,2)}\chi_k^{(2,3)} \end{bmatrix} \right\| \left\| \begin{bmatrix} \chi_k^{(1,2)}\chi_k^{(2,3)}\chi_k^{(3,4)} \\ \chi_k^{(1,2)}\chi_k^{(2,3)}\chi_k^{(3,4)}\chi_k^{(4,5)} \\ \chi_k^{(1,2)}\chi_k^{(2,3)}\chi_k^{(3,4)}\chi_k^{(4,5)}\chi_k^{(5,6)} \end{bmatrix} \right\|}$$

Thus, the complex scalar ambiguity of $r_k e^{j\alpha_k}$ in (14) causes no ambiguity in the direction cosine estimates.

### 3.5. Azimuth & Elevation Angle Estimates

From the direction-cosine estimates derived above, the $k$th signal's azimuth and elevation arrival angles can be estimated as:

$$\hat{\theta}_k = \sin^{-1}\sqrt{\hat{u}_k^2 + \hat{v}_k^2} = \cos^{-1}\hat{w}_k$$

$$\hat{\phi}_k = \tan^{-1}\frac{\hat{v}_k}{\hat{u}_k}$$

Note that once the $\{\chi_k^{(j,j+1)}, \quad j = 1, \ldots, 5\}$ are paired, the azimuth and elevation estimates are also automatically matched with no additional processing.

A basic calibration method and a simple remedy will also be presented in the journal version of this work to illustrate the possibility of modifying the foregoing algorithm to accommodate electromagnetic vector-sensor mis-orientation.

## 4. SIMULATIONS

The simulation results presented in figure 1 verifies the efficacy of this novel close-form direction finding algorithm for arbitrarily spaced electromagnetic vector-sensors at unknown locations. Two closely-spaced equal-power uncorrelated narrowband sources impinge upon a 13-element irregularly spaced three-dimensional array of vector-sensors. This array may be considered as a 9-element non-uniformly spaced cross-shaped array with elements at the Cartesian coordinates $\frac{\lambda}{2} \times \{(0,0,0), (\pm 1,0,0)(\pm 2.7,0,0), (0,\pm 1,0), (0,\pm 2.7,0)\}$ plus a 4-element square array with elements at the Cartesian coordinates $\frac{\lambda}{2} \times \{(\pm 4, \pm 4, 1)\}$. The two closely-spaced equal-power uncorrelated narrowband sources have the following parameter values: $\theta_1 = 30.93°, \phi_1 = 37.09°$, $\theta_2 = 50.08°, \phi_2 = 39.71°$. (that is, the first source has $u_1 = 0.41$ and $v_1 = 0.31$ and the second source has $u_2 = 0.59$ and $v_2 = 0.49$.) The polarization states are $\gamma_1 = 45°, \eta_1 = 90°$, $\gamma_2 = 45°, \eta_2 = -90°$. The SNR is defined relative to each source. 200 snapshots are used in each of the 500 independent Monte Carlo simulation experiments.

The composite RMS standard deviation plotted is computed by taking the square root of the mean of the respective samples variances of $\hat{u}$ and $\hat{v}$. The estimation bias (not shown) is about an order of magnitude smaller than the estimation standard deviation and follows a similar trend. Note that $u_2 - u_1 = v_1 - v_2 = 0.18$; thus, the two sources would be resolved and identified with high probability if both the estimation standard deviation and the bias are under approximately 0.05. The proposed ESPRIT-based

Figure 1: RMS standard deviation of $\{\hat{u}, \hat{v}\}$ versus SNR.

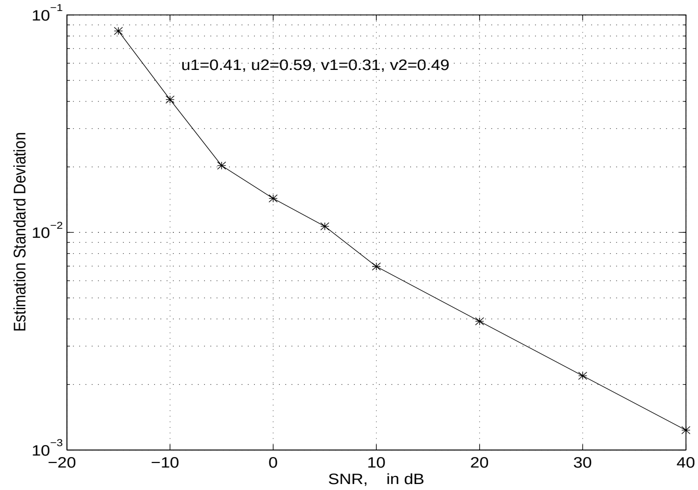


algorithm successfully resolves these closely-spaced sources for all SNR's at or above $-12$ dB. Above these SNR resolution thresholds, estimation standard deviation and bias both decrease fairly linearly with increasing SNR dB values.

## 5. BIBLIOGRAPHY

[1] R. O. Schmidt, "Multiple Emitter Location and Signal Parameter Estimation," *RADC Spectral Estimation Workshop* 1979.

[2] R. Roy and T. Kailath, "ESPRIT-Estimation of Signal Parameters Via Rotational Invariance Techniques," *IEEE Trans. Acoustics, Speech, Signal Processing*, 7/89, pp. 984-995.

[3] D. J. Farina, "Superresolution Compact Array Radiolocation Technology (SuperCART) Project," Flam & Russell Technical Report, no. 185, Nov. 1990.

[4] A. Nehorai and E. Paldi, "Vector-Sensor Array Processing for Electro-magnetic Source Localization," *IEEE Trans. Signal Processing*, 2/94, pp. 376-398.

[5] J. Li, "Direction and Polarization Estimation Using Arrays with Small Loops and Short Dipoles," *IEEE Trans. Antennas & Propagation*, 3/93., pp. 379-387.

[6] B. Champagne, "Adaptive Eigendecomposition of Data Covariance Matrices Based on First-Order Perturbations," *IEEE Trans. Signal Processing*, pp. 2758-2770, 10/94.

[7] K. T. Wong and M. D. Zoltowski, "High Accuracy 2D Angle Estimation with Extended Aperture Vector Sensor Array," *IEEE Intl. Conf. Acoustics, Speech, Signal Processing*, vol. 5, pp. 2789-2792, 1996.

[8] K. T. Wong & M. D. Zoltowski, "Uni-Vector-Sensor ESPRIT for Multi-Source Azimuth-Elevation Angle-Estimation," *IEEE Antennas & Propagation Society Intl. Symp.*, pp. 1368-1371, 1996.

[9] M. D. Zoltowski & K. T. Wong, "Polarization Diversity & Extended-Aperture Spatial Diversity to Mitigate Fading-Channel Effects with a Sparse Array of Electric Dipoles or Magnetic Loops," *IEEE Intl. Vehicular Technology Conf.*, pp. 1163-1167, 1997.

[10] K. T. Wong & M. D. Zoltowski, "Polarization-Beamspace Self-Initiating MUSIC for Azimuth/Elevation Angle Estimation ," accepted by *IEE Radar'97 Intl. Radar Conference*.

[11] K. T. Wong & M. D. Zoltowski, "Uni-Vector-Sensor ESPRIT for Multisource Azimuth, Elevation, and Polarization Estimation," *IEEE Trans. Antennas & Propagation*, vol. 45, no. 10, pp. 1467-1474, Oct. 1997.